Impact of Amplified Spontaneous Emission on the Travelling Wave Semiconductor Optical Amplifier Performance

A. Abd El Aziz, Engy K. El Nayal, and Moustafa H. Aly
Photonic Research Laboratory (PRL)
Arab Academy for Science and Technology (AAST)
Alexandria, Egypt
(drmosaly@gmail.com)

A.K. AboulSeoud
Faculty of Engineering
University of Alexandria
Alexandria, Egypt
(Aboul_Seoud_35@yahoo.com)

W. P. Ng
Senior Member, IEEE
Northumbria University
Newcastle upon Tyne
UK
(wai.pang.ng@ieee.org)

***Abstract*—The most important characteristic that affects the travelling wave-semiconductor optical amplifier (TW-SOA) performance is the amplified spontaneous emission (ASE) noise. This paper presents the SOA operation using the segmentation model that utilizes the rate equation employing the ASE noise. The impact of ASE noise on the total SOA gain response in absence and presence of input signals is investigated. Also the impact of ASE noise on SOA length for a single pulse and a packet of pulses and making comparison between them are introduced. As well as studying the dependence of gain uniformity on SOA length under the influence of ASE noise is clarified by calculating the gain standard deviation.**

Keywords—carrier density, semiconductor optical amplifier (SOA), amplified spontaneous emission (ASE) and gain response

I. INTRODUCTION

The ever increasing speed and capacity requirements are the driving forces behind the development of photonic devices that can perform different functions within an optical system in order to overcome the speed bottleneck optical-electrical-optical (O-E-O) conversion [1, 2]. Semiconductor optical amplifier (SOA) is one of these key devices that fiber optics and optical wireless communications rely on [3, 4]. Due to the SOA strong non-linear characteristics, wavelength flexibility, short response time and easily integration with electronic and optical devices, it is not only used as a simple gain unit [5-7]. It is used in all-optical networks for clock extraction, all-optical switching, wavelength conversion, all-optical gates and optical processing. On the other hand, SOA is also a very promising device for free space optical (FSO) communication systems. In the receiver end of a FSO link, SOAs are used to decrease the received signal fluctuations produced by atmospheric turbulence. The impact of such turbulence results in direct limitations to the transmission distance and system capacity (i.e. reduces system performance) of the FSO link [8]. When the SOA is saturated by the turbulent signal, it suppresses the induced scintillation and reduces the intensity fluctuations [8].

One of the most crucial factors for the performance evaluation of transmission systems featuring SOAs is the amplified spontaneous emission (ASE) noise [9]. The main source of noise in the optical field in a semiconductor optical gain medium is the spontaneous emission of photons by recombination of electron–hole pairs. A number of schemes have been proposed to evaluate the optical signal to noise ratio (OSNR) and the noise figure (NF) of SOAs theoretically and experimentally [10-12]. Different approaches have also been used to describe the effects of ASE noise on the quality of the optically generated electrical signals theoretically [9].

This paper addresses the impact of ASE noise and its effect on the behavior and the performance of SOA. The total rate equations employing the ASE noise are presented. The impact of ASE noise on the signal gain at different SOA lengths is also investigated in this paper. No work has been reported on the SOA for improving the gain uniformity under the influence of ASE noise. For that reason, the gain standard deviation which measures the SOA gain uniformity at high speed data rates is presented [13]. The uniformity of the output signals is compared to highlight the dependence of the SOA performance on ASE noise.

This paper is organized as follows; in section II, the mathematical TW-SOA segmentation model that accounts for the ASE noise is presented. In section III, the difference of the total SOA gain response and its dependence on the noise gain either in absence or presence of input signals with the effect of ASE noise are studied. Special attention is given to the influence of noise on the SOA's length in case of single Gaussian pulse and a packet of Gaussian signals as an input to SOA are studied. Thus the gain standard deviation is measured to study the dependence of SOA gain uniformity on length. In section IV, the findings of this investigation are concluded.

II. MATHEMATICAL MODEL

When light is injected into the SOA, changes occur in the carrier and photon densities within the active region which can be described using the rate equations. These rate equations in small segments in a Bulk InGaAsP/InP SOA are iteratively calculated while taking the carrier density change in account [14]. The dynamic equation for

978-1-4799-1188-2/13/$31.00 ©2013 IEEE

the change in the carrier density within the active region is given by [13]:

$$\frac{dN}{dt} = \frac{I}{q.V} - (A.N + B.N^2 + C.N^3) - \frac{\Gamma.g.P_{av}.L}{V.h.f} - \frac{2\Gamma}{h\,H\,W}\sum_{j=0}^{N_m-1}\frac{g_{noise}.k_j}{v_j}P_{ASE} \quad (1)$$

where I is the DC current injected to the SOA, q is the electron charge, Γ is the confinement factor, K_j is the filter factor, h is the Plank's constant, f is the light frequency and V is the active volume of the SOA.

The active volume is determined by $V = L \times W \times H$ where L is the length of the SOA, W and H are the width and the thickness of the active region, respectively. A is the surface and defect recombination coefficient while B and C are the radiative and Auger recombination coefficients, respectively.

The material gain coefficient g depends on both the carrier density N and the input signal wavelength λ is given by:

$$g = a_1(N - N_o) - a_2(\lambda - \lambda_N)^2 + a_3(\lambda - \lambda_N)^3 \quad (2)$$

where a_1 is the differential gain parameter, a_2 and a_3 are empirically determined constants, N_o is the carrier density at the transparency point. λ_N is the peak gain wavelength. The peak gain wavelength is given by:

$$\lambda_N = \lambda_o - a_4(N - N_o) \quad (3)$$

where λ_o is the peak gain wavelength at transparency and a_4 denotes the empirical constant.

The average output power P_{av} over the length of the SOA becomes [13]:

$$P_{av} = \frac{1}{L}\int_0^L P_{in}.\,G\;\,dz \quad (4)$$

where P_{in} is the input signal power and G is the total gain of an optical wave experienced at the location z of an SOA. The total gain can be calculated according to:

$$G = e^{g_T \cdot z} \quad (5)$$

where g_T is the net gain coefficient and is defined by:

$$g_T = \Gamma.g - \propto_s \quad (6)$$

where α_s is the internal waveguide scattering loss.

P_{ASE} is the amplified spontaneous emission noise power (Watt) and it obeys the travelling-wave equation:

$$\frac{dP_{ASE}}{dz} = (\Gamma g_{noise} - \alpha_s)P_{ASE} + R_{sp} \quad (7)$$

where R_{sp} represents the local spontaneously generated noise and is given by:

$$R_{sp} = \Gamma.g_{noise}.\Delta v_m.h.v_j \quad (8)$$

The spontaneous emission distributes itself continuously over a relatively wide band of wavelengths with random phases between adjacent wavelength components. These noise photons frequencies v_j are given by:

$$v_j = v_c + j\,\Delta v_m, \quad j = 0 \ldots (N_m - 1) \quad (9)$$

where N_m is a positive integer, v_c is the cut-off frequency and it is given by $v_c = \frac{E_{g0}}{h}$ and Δv_m is the longitudinal mode frequency spacing which is:

$$\Delta v_m = \frac{c}{2\,n_{eq}\,L} \quad (10)$$

where c is the speed of light in vacuum and n_{eq} is the equivalent index of the amplifier waveguide.

The bandgap energy E_{g0} with no injected carriers is given by the quadratic approximation:

$$E_{g0} = q\,(a + b\,y + c\,y^2) \quad (11)$$

where a, b and c are the quadratic coefficients and y is the molar fraction of Arsenide in the active region.

The above equations shown in this section are carried out via Matlab™ to investigate the gain response of the SOA model considering ASE noise while employing the segmentation method. This model involves dividing the SOA into fifty segments.

The physical SOA parameters used for the model are given in Table I [15].

TABLE I. PHYSICAL PARAMETERS USED IN THIS WORK.

Parameter	Value
Carrier density at transparency (N_0)	1.4×10^{24} / m^3
Wavelength at transparency (λ_0)	1605 nm
Initial carrier density (N_i)	3×10^{24} / m^3
Internal waveguide scattering loss (α_s)	40×10^{2} / m
Differential gain (a_1)	2.78×10^{-20} / m^2
Gain constant (a_2)	7.4×10^{18} / m^3
Gain constant (a_3)	3.155×10^{25} / m^4
Gain peak shift coefficient (a_4)	3×10^{-32} m^4
SOA Length (L)	500 µm
SOA width (W)	3 µm
SOA height (H)	80 nm
Confinement factor (Γ)	0.3
Filter factor (k_j)	1
Molar fraction of Arsenide in the active region (y)	0.892
Bandgap energy quadratic coefficient (a)	1.35
Bandgap energy quadratic coefficient (b)	-0.775
Bandgap energy quadratic coefficient (c)	0.149
Surface and detect recombination coefficient (A)	3.6×10^{8} / s
Radiative recombination coefficient (B)	5.6×10^{-16} m^3/s
Auger recombination coefficient (C)	3×10^{-41} m^6/s
Equivalent refractive index (n_{eq})	3.5
Facet reflectivities (R_1, R_2)	0

III. RESULTS AND DISCUSSIONS

A. SOA in the absence of input signals

The segmentation model in this paper is proposed in order to accurately study the impact of the SOA parameters and the resultant ASE noise on the carrier density and SOA gain. This study helps to investigate the effect of the ASE noise on the SOA performance for a given application. The model is based on a unidirectional (forward) bulk travelling wave SOA (TW-SOA) (i.e. has negligible reflectivity at the end facets). All results are based on the SOA physical parameters in Table I. The SOA gain response with and without the impact of the ASE noise is first introduced in the absence of input signals in Fig. 1.

The gain of the SOA rapidly increases till it reaches a steady state value within t_{bias} ~1 ns due to biasing. A large number of electrons in the valence band will gain enough energy to overcome the energy gap, increasing the carrier density and hence the SOA total gain.

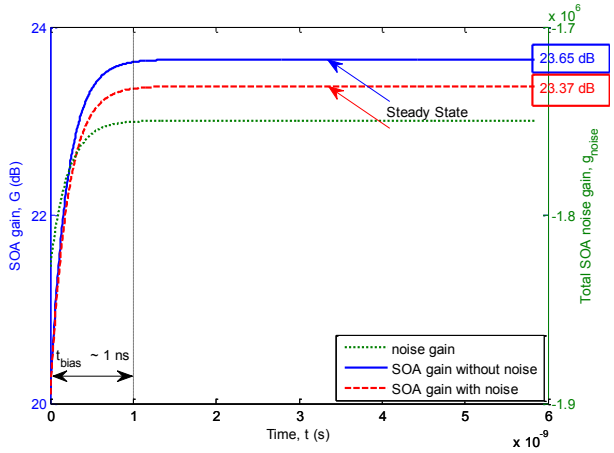

Fig. 1. The total gain and the noise gain responses of the SOA with no input signal.

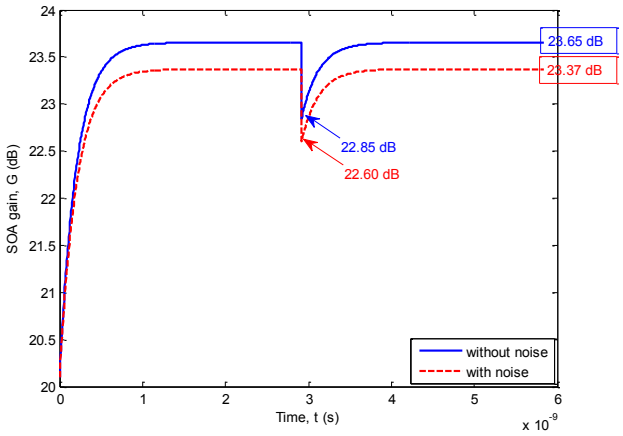

Fig. 2. The total gain response of the SOA due the input Gaussian pulse.

This gain is 23.65 dB (solid line) as seen from Fig. 1, however; this steady state value is only 23.37 dB (dashed line) due to the presence of the ASE noise. Although the gain response is similar on both cases, the number of excited electrons in the conduction band (i.e. carrier density) is lower in case of ASE noise due to the spontaneous emission process that takes place. Such response can be further explained from equation (1) which defines the carrier density rate of change. Only the 1st and 2nd terms of (1) are considered in the absence of the input signal (which appears in the 3rd term) and the ASE noise (which appears in the 4th term). The equation is balanced at a constant value of N. On the other hand, by subtracting the 4th term due to ASE noise, the equation is balanced at a lower N (i.e lower SOA gain). The 4th term depends on the noise gain g_{noise} that is shown in Fig. 1 (dotted line). As expected, one can see from the figure that g_{noise} has a corresponding response to the SOA gain. The spontaneous emission fundamentally originates from the carriers injected into the active region by the biasing current.

B. SOA in the Presence of Input Signals

In order to understand the impact of ASE noise on the SOA gain response, an input signal is applied to the SOA. In Fig. 2, this gain response is illustrated with and without ASE noise when a short input Gaussian pulse with 1 mW peak power and width of 1.1667 ps is applied to the SOA at the same time.

The injection of the Gaussian signal results in an instant drop in the SOA gain (i.e. carrier density) due to the interaction of the incident pulse with the excited electrons in the conduction band during its propagation along the SOA length. This gain depletion is dependent on the power and wavelength of the input signal. The gain starts to recover back to the steady state value after the exit of the propagating pulse from the SOA.

From Fig. 2, it can be seen that the gain depletion due to ASE noise reach a lower value (i.e. lower gain achieved by the input signal) compared to noise free propagation.

C. Impact of the ASE noise on the SOA length

The direct impact of the ASE noise on the SOA gain was highlighted in the previous section. This gain is dependent on several parameters such as the SOA length, the biasing current and the input parameters. This section studies the gain affected by the ASE noise for any SOA length at different biasing current. The input parameters in this study are fixed at 1 mW peak power and at a wavelength of 1550 nm. The SOA length range investigated in this paper is 450 µm < L < 1000 µm where the most commonly used experiments are executed [16]. SOAs with lengths shorter than 450 µm do not show significant effect of ASE noise on the SOA gain due to the limited propagating time for amplification and hence ASE noise can be neglected. In order to present the ASE noise at such short distances, larger currents are required to bias the SOA which is experimentally limited to ~ 500 mA [17].

From Fig. 3 (a) one can see the impact of the ASE noise on the SOA gain which is depicted for the entire range of SOA lengths at 150 mA with and without the effect of the noise. The figure shows that the gain decreases at longer SOAs for both curves. The reason for such response is that the bias current is maintained 150 mA and therefore, at longer length, the number of electrons per unit length is smaller at longer SOAs (i.e. lower current density). As for L < 450 µm, higher biasing currents are required to increase the SOA gain at longer SOAs. Fig. 3 (a) shows that the ASE noise decreases the SOA gain at all investigated lengths. This gain drop is measured and illustrated at 150, 200 and 250 mA in Fig. 3 (b).

As shown in Fig. 3 (b), this gain drop is lower at longer SOAs. This response is expected due to the lower noise gain which is dependent on N (see equation (1)) and hence smaller differences from the noise free SOA. For that reason, the highest gain drops are seen at 450 µm while the lowest are at 1000 µm for all bias currents.

At higher bias currents, more electrons overcome the energy gap to reach the conduction band and therefore, the carrier density and total gain increase. The highest gain drops (i.e. maximum ASE noise impact) are 11.16

dB, 13.01 dB and 11.61 dB which correspond to 6.035 %, 2.559 % and 0.9904 % percentage gain drop at 150, 200 and 250 mA, respectively. On the other hand, the lowest gain drops for the same biasing currents are -12.3 dB, 1.045 dB and -7.496 dB that compatible with 3.358 %, 1.263 % and 0.05143 % respectively.

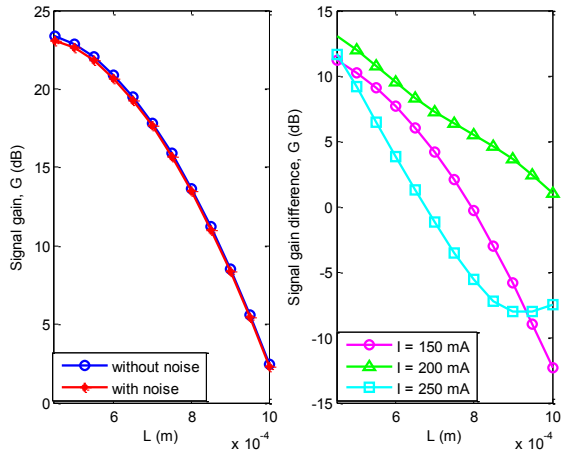

(a) (b)

Fig. 3. (a) The signal gain response as a function of the SOA length. (b) The significant difference of the signal gain at I = 150 mA, 200 mA, 250 mA.

The investigation is further carried out to study the impact of the ASE noise on the SOA gain not only for a single propagating pulse but for a sequence of the pulses or a packet. The packet consists of 10 Gaussian pulses identical to the one investigated earlier and is also propagating at 1550 nm. All pulses are separated by 100 ps (i.e. 10 Gb/s data rate) for a packet duration of 1 ns. The response of the SOA gain to the input propagating packet is displayed in Fig. 4.

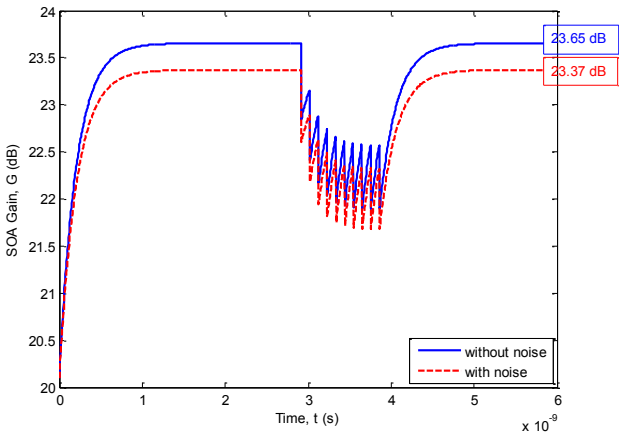

Fig. 4. The SOA gain response when injected with a burst input pulse trains.

When the first pulse in the packet enters the SOA at time ~ 3 ns, gain depletion occurs due to the interaction of the input pulse with the excited electrons in the conduction band. Due to the slow recovery of the SOA gain, the next pulse enters the SOA before its full recovery. A further gain depletion is introduced because of the second pulse. This process continues until the last pulse exits the SOA. Each pulse therefore achieves different gain value (gain drops to different levels) that results in patterning effect and signal distortion [18]. For that reason, it is important to investigate the impact of the ASE noise on two factors in case packet propagation. These factors are the average gain for the input pulses (i.e. the average packet gain) and the output gain uniformity [19]. The gain response is plotted in Fig. 4 at noise free propagation and with the ASE noise in order to investigate its impact. Once again a drop in the gain at all times is seen due to the effect of the noise. The average gain drop for the packet when ASE is considered is depicted in Fig. 5 at all investigated SOA lengths at different bias currents.

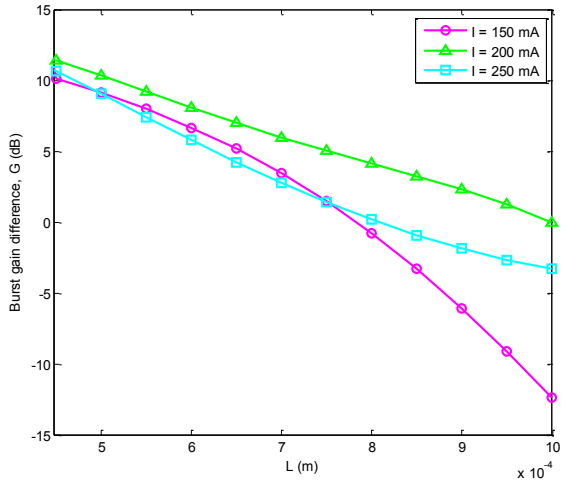

Fig. 5. The significant difference of the average burst gain at I = 150 mA, 200 mA, 250 mA.

Comparing this figure to Fig. 3 (b) with the impact of ASE noise on the single propagating pulse, similar responses are observed at the three investigated bias current values. However, these gain drops are less in case of the packet propagation; i.e. 10.13, 11.38 and 10.64 dB maximum drops at L = 450 µm which matches with 5.598 %, 2.404 % and 1.156 % percentage gain drop and -12.37, -0.03 and -3.29 dB minimum drops at L =1000 µm that agree with 3.336 %, 1.173 % and 0.1648 % for 150, 200 and 250 mA, respectively. The average gains of the pulses within the packet are less than the gains of the single propagating pulse with and without the ASE noise. This is due to the further gain depletions to the SOA gain in case of packet propagation.

In order to measure the gain uniformity of the output pulses, the gain standard deviation is introduced which is given by [13]:

$$\sigma = \sqrt{\frac{1}{np}\sum_{x=1}^{np}(G_x - G_{av})^2} \qquad (12)$$

where np is the number of successive input pulses launched into the SOA, G_x is the gain achieved by each input pulse and G_{av} is the average gain of all input pulses. To study the dependence of the SOA gain uniformity on the SOA length and the corresponding impact of the ASE noise, the gain standard deviation is calculated from equation (12) and plotted in Fig. 6 (a). As explained earlier, at higher lengths, the average packet gain decreases and hence the gain standard deviation. This

explains the highest and lowest gain uniformities at L = 450 μm and L = 1000 μm lengths, respectively. The maximum value of σ (i.e. least gain uniformity) is 10.64 and 11.01 dB with and without the impact of the ASE, respectively, while these values are -21.41 and -21.17 at maximum gain uniformity. Although the ASE noise has caused the average gain of the input pulses within the package to drop, the gain standard deviation has decreased and therefore, there is an improvement in the output gain uniformity. This improvement is displayed in Fig. 6 (b) at all SOA lengths at the 150, 200 and 250 mA currents.

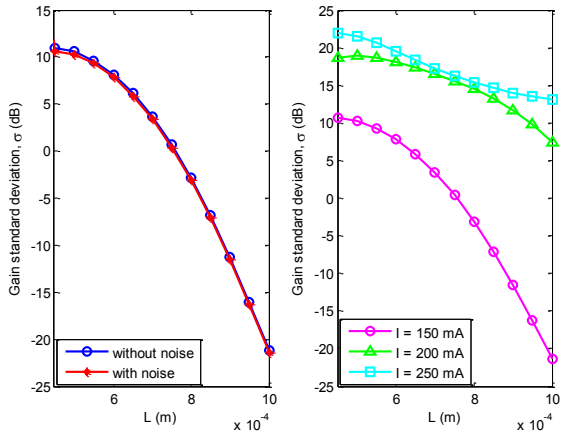

(a) (b)

Fig. 6. (a) Gain standard deviation against SOA length at I = 150 mA. (b) Gain standard deviation as a function of SOA length at I = 150 mA, 200 mA, 250 mA.

IV. CONCLUSION

This paper has presented the segmentation mathematical model that describes the TW-SOA features utilizing the complete rate and propagation equations necessary for the SOA operation. This model investigates the effect of the ASE noise on the total gain response in absence and presence of the input signals and also the noise effect on SOA length.

It is concluded that the cause of the drop in the gain is due to the electrons accumulated in the conduction band by population inversion are decreased by noise photons. This decreases the number of available electrons to be stimulated by the signal.

Finally, SOA model and dynamic behavior are important tools that allow the SOA designer to develop optimized devices. As in this work, the improvement in the output gain uniformity is achieved when the gain standard deviation has decreased at worked SOA lengths.

REFERENCES

[1] D. Adami, S. Giordano, M. Pagano, and L. Gustavo Zuliani, "MCP-RWA: A novel algorithm for QoT-guaranteed online provisioning in Photonic Networks," in Ultra-Modern Telecommunications and Control Systems and Workshops (ICUMT), 2010 International Congress on, pp. 141-147, 2010.

[2] C. Schubert, J. Berger, S. Diez, H. J. Ehrke, R. Ludwig, U. Feiste, C. Schmidt, H. G. Weber, G. Toptchiyski, S. Randel, and K. Petermann, "Comparison of interferometric all-optical switches for demultiplexing applications in high-speed OTDM systems," Lightwave Technology, Journal of, vol. 20, pp. 618-624, 2002.

[3] K. Morito, J. Leuthold, and H. Melchior, "Dynamic analysis of MZI-SOA all optical switches for balanced switching," in Integrated Optics and Optical Fibre Communications, 11th International Conference on, and 23rd European Conference on Optical Communications (Conf. Publ. No.: 448), vol.2, pp. 81-84, 1997.

[4] T. Saitoh and T. Mukai, "Traveling-wave semiconductor laser amplifiers for optical communications systems," in Global Telecommunications Conference, 1990, and Exhibition. 'Communications: Connecting the Future', GLOBECOM '90., IEEE, vol.2, pp. 1274-1280, 1990.

[5] M. J. Connelly, "Semiconductor optical amplifiers," New York: Springer, Verlag, 2002.

[6] N.K. Dutta and Q. Wang, "Semiconductor optical amplifiers," World Scientific Publishing, Singapore, 2006 (Chapter 8) and references therein.

[7] R. Ramaswami and N. Sivarajan, "Optical network – a practical perspective," 2 ed. USA: Morgan Kaufmann, 2002.

[8] Mohammad Abtahi, Pascal Lemieux, Walid Mathlouthi, and Leslie Ann Rusch, "suppression of turbulence-induced scintillation in free-space optical communication systems using saturated optical amplifiers", Journal of Lightwave Technology, Vol. 24, NO. 12, December 2006.

[9] Guohua Qi, Joe Seregelyi, Stéphane Paquet and J. Claude Bélisle, "Effects of amplified spontaneous emission noise of optical amplifiers on the phase noise of optically generated electrical signals," Proc. SPIE 5971, Photonic Applications in Nonlinear Optics, Nanophotonics, and Microwave Photonics, Oct 2005.

[10] Y. Said, H. Rezig and A. Bouallegue, "Analysis of noise effects in long semiconductor optical amplifiers," The Open Optics Journal, 2008.

[11] Guido Giuliani, and Davide D'Alessandro, "Noise analysis of conventional and gain-clamped semiconductor optical amplifiers," Journal of Lightwave Technology, VOL. 18, NO. 9, Sep 2000.

[12] E. Staffan Björlin, and John E. Bowers, "Noise figure of vertical-cavity semiconductor optical amplifiers," IEEE Journal of Quantum Electronics, Vol. 38, No. 1, Jan 2002.

[13] A. A. El Aziz, W. P. Ng, Z. Ghassemlooy, M. H. Aly, R. Ngah, and M. F. Chiang, "Impact of signal wavelength on the semiconductor optical amplifier gain uniformity for high speed optical routers employing the segmentation model," presented at Information Sciences Signal Processing and their Applications (ISSPA), 10th International Conference, May 2010.

[14] M. Hattori, K. Nishimura, R. Inohara, and M. Usami, "Bidirectional data injection operation of hybrid integrated SOAMZI all-optical wavelength converter," Journal of Lightwave Technology, vol. 25, pp. 512-519, 2007.

[15] VPIsystems, VPI transmission maker and VPI component maker: photonic modules reference manual, 2001.

[16] Gutierrez-Castrejon, R., Schares, L. , Occhi, L., Guekos, G. "Modeling and measurement of longitudinal gain dynamics in saturated semiconductor optical amplifiers of different length," Quantum Electronics, IEEE Journal, 2000.

[17] Prashant P. Baveja, Aaron M. Kaplan, Drew N. Maywar, and Govind P. Agrawal, "Pulse amplification in semiconductor optical amplifiers with ultrafast gain-recovery times," Proc. of SPIE Vol. 7598, 2010.

[18] J. Xu, X. Zhang, and J. Mork, "Investigation of patterning effect in ultrafast SOA-based optical switches," in Lasers and Electro-Optics 2009 and the European Quantum Electronics Conference. CLEO Europe - EQEC 2009. European Conference on, pp. 1, 2009.

[19] Abd El Aziz, A., Ng, W. P., Ghassemlooy, Z., Aly, M., and Ngah, R., "Employing wavelength diversity to improve SOA gain uniformity," The 15th European Conference on Networks and Optical Communications (NOC 2010), pp. 301-306, Faro-Algarve, Portugal, 8-10 June 2010.